A General Approach for Calculating Speciation and Poising Capacity of Redox Systems with Multiple Oxidation States: Application to Redox Titrations and the Generation of pε−pH Diag...

ARTICLE *in* JOURNAL OF CHEMICAL EDUCATION · AUGUST 2002

Impact Factor: 1.11 · DOI: 10.1021/ed079p1135

1 AUTHOR:

Whitney King
Colby College
21 PUBLICATIONS **1,268** CITATIONS

A General Approach for Calculating Speciation and Poising Capacity of Redox Systems with Multiple Oxidation States: Application to Redox Titrations and the Generation of pε–pH Diagrams

D. Whitney King
Department of Chemistry, Colby College, Waterville, ME 04901; *dwking@colby.edu*

Providing detailed descriptions of complex systems in terms of proton and redox equilibria is a challenge faced by many chemists. In the environmental chemistry field a number of comprehensive texts have advanced the use of pH and pε as master variables in defining the geochemistry of aquatic systems in equilibrium with the atmosphere and soils *(1–3)*. These variables define the classic pε–pH diagram as described by Sillén in this *Journal (4)*. Derivatives of concentration with respect to pH and pε define proton buffer capacity and electron poising capacity, respectively. These concepts build directly on the conventional quantitative analysis curriculum emphasizing acid–base, metal complexation, and redox equilibria. Analysis of relevant geochemical systems to produce pε–pH diagrams is interesting for many students and nicely integrates many of the concepts introduced in quantitative analysis.

This paper presents a general approach for calculating redox titrations, speciation, and poising capacity of systems with multiple oxidation states. Previously, we described in this *Journal (5)* a general approach for calculating polyprotic acid speciation and buffer capacity. Also in this *Journal,* de Levie *(6)* described a general approach for calculating redox buffer strength. I will show how the two approaches can be used to readily generate pε–pH diagrams using standard spreadsheet software (Excel).

General Equations for Proton Equilibria

I will begin with a short review of the general approach for calculating polyprotic acid speciation and buffer capacity. The approach is based on the calculation of the degree of protolysis, or relative fraction (α_j) for each acid species

$$\alpha_{H_nA},\ \alpha_{H_{n-1}A^{1-}},\ \alpha_{H_{n-2}A^{2-}},\ \ldots,\ \alpha_{H_{n-j}A^{j-}} \qquad (1)$$

where the order of each dissociation is indicated by the index j, which ranges from 0 to n. The degree of protolysis (α_j) is simply the ratio of the concentration of a particular acid species ($H_{n-j}A^{j-}$) to the total acid concentration. Calculation of these terms is treated in most quantitative analysis texts (*7*) and is provided in the general form in eqs 2 and 3

$$\alpha_j = \frac{\left(\prod_{i=0}^{j} K_i\right)(H^+)^{n-j}}{d} \qquad (2)$$

$$d = \sum_{j=0}^{n}\left[\left(\prod_{i=0}^{j} K_i\right)(H^+)^{n-j}\right] \qquad (3)$$

where $K_0 = 1$. As an example, α_0 for a diprotic acid ($n = 2$) is defined as

$$\alpha_0 = \frac{(H^+)^2}{(H^+)^2 + K_1(H^+) + K_1K_2} \qquad (4)$$

where K_1 and K_2 are the first and second acid dissociation constants, respectively. Parentheses denote the activity of the enclosed species, which can be considered equal to concentration for many applications.

From the α_j function follow several other useful parameters for describing acid–base systems. The degree of dissociation of an acid (η) is the ratio of the number of moles of protons dissociated to the total moles of acid. This parameter can be calculated as a function of pH from the weighted sum of all α_j terms. For $n = 2$,

$$\eta = \frac{\text{moles of } H^+ \text{ dissociated}}{\text{moles of acid}} = \sum_{j=0}^{n} j\alpha_j = \alpha_1 + 2\alpha_2 \qquad (5)$$

A plot of η as a function of pH is shown in Figure 1. The derivative of η with respect to pH describes the buffer capacity of the weak acid (β), which is also defined as the derivative of added strong acid or base (C_s) to the change in pH of a weak acid or base *(5, 8)*.

$$\beta = \mathrm{TM}\frac{d\alpha_1}{d(pH)} + 2\mathrm{TM}\frac{d\alpha_2}{d(pH)} + \ldots + n\mathrm{TM}\frac{d\alpha_n}{d(pH)} \qquad (6a)$$

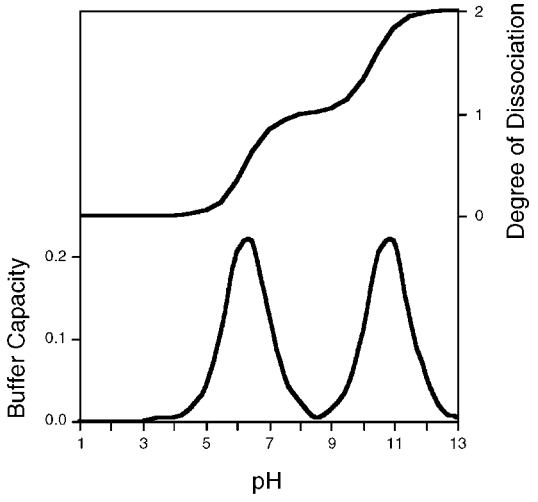

Figure 1. Degree of dissociation (η) and buffer capacity (β) of carbonic acid.

$$\beta = \left| \frac{dC_s}{d(pH)} \right| = 2.303TM\sum_{j=1}^{n}\sum_{i=0}^{j-1}(j-i)^2\alpha_j\alpha_i \qquad (6b)$$

For $n = 2$,

$$\beta = 2.303TM(\alpha_0\alpha_1 + 4\alpha_0\alpha_2 + \alpha_1\alpha_2) \qquad (6c)$$

The magnitude of the function is determined by the total moles of weak acid (TM).

Applications to Redox Systems

The above approach for calculating α, η, and β for polyprotic systems is equally valid when considering reversible redox reactions. The condition of reversibility is met for many redox systems. Excellent examples of reversible reactions can be found in the redox titration chapters of most quantitative analysis texts. In addition, many reactions that are not reversible on a laboratory time scale are reversible on a geochemical time scale (e.g., the reduction of Fe^{III} and SO_4^{2-} by organic carbon). In this case, the approach that will be described will provide a tool to predict equilibrium conditions in geochemical systems. As an example, this capability is necessary to evaluate the effect of redox manipulation of water systems. Redox manipulation is one of the remediation tools used to control groundwater contamination. In natural systems, bacteria enhance the rate of redox reactions by acting as biological redox catalysts. This promotes redox reversibility in many natural systems. For a more complete discussion of natural water redox equilibria see refs *2*, *3*, and *9*.

General Equations for Redox Equilibria

First, consider a general system with multiple oxidation states. The most reduced species, O_0, will be oxidized in a series of one-electron steps to form the oxidized species.

$$O_0,\ O_1^{+},\ O_2^{2+},\ \ldots,\ O_j^{j+} \qquad (7)$$

Each step in the oxidation series is defined by an equilibrium constant

$$K_j = \frac{\left(O_j^{j+}\right)\left(e^-\right)}{\left(O_{j-1}^{+j-1}\right)} \qquad (8)$$

where (e^-) is the activity of the electron, often described by the pε ($pε = -\log(e^-)$) or E, which are proportional to electron free energy. The equilibrium constant is directly related to standard redox potentials *($E°$)* and pε°,

$$-\log K_j = n(pε°) = \frac{nF}{2.303RT}E° \text{ and } pε = \frac{F}{2.303RT}E \qquad (9)$$

and K_0 is defined as one. Having defined K_j, the distribution function (α_j) for different oxidation states follows from eqs 2 and 3.

$$\alpha_j = \frac{\left(\prod_{i=0}^{j} K_i\right)(e^-)^{n-j}}{d} \qquad (10)$$

$$d = \sum_{j=0}^{n}\left[\left(\prod_{i=0}^{j} K_i\right)(e^-)^{n-j}\right] \qquad (11)$$

where the electron activity replaces the proton activity in the expressions. Similarly, the expressions for the degree of oxidation (η_0) and poising (buffer) capacity (ρ) of the redox system can be calculated.

$$\eta_0 = \frac{\text{moles of } e^-}{\text{moles of reductant}} = \sum_{j=0}^{n} j\alpha_j \qquad (12)$$

$$\rho = TR\frac{d\alpha_1}{d(pε)} + 2TR\frac{d\alpha_2}{d(pε)} + \ldots + nTR\frac{d\alpha_n}{d(pε)} \qquad (13a)$$

$$\rho = \left| \frac{dC_{ox}}{d(pε)} \right| = 2.303TR\sum_{j=1}^{n}\sum_{i=0}^{j-1}(j-i)^2\alpha_j\alpha_i \qquad (13b)$$

In this case, C_{ox} is defined as the moles of added oxidant and TR is the total concentration of the reduced species. I have selected pε as a master variable in the general redox reactions owing to the clear analogy with pH and acid–base systems. This can cause some confusion, since free electrons do not exist in solution. However, it follows from eq 8 that the electron activity and also free energy are defined in any system in which the activities of reduced and oxidized species are defined.

As a practical matter, the maximum number of electron dissociations is 8 (9 different oxidation states). Therefore, it is convenient to implement eqs 7–13 for $j = 8$. The supplemental material provides example expressions for α_j, η_0, and ρ.[ω] A spreadsheet application such as Excel makes it easy to calculate α_j, η_0, and ρ as a function of pε.

Figure 2 provides an example for the manganese system

$$Mn^0 \xrightarrow{-2e} Mn^{II} \xrightarrow{-e} Mn^{III} \xrightarrow{-e} Mn^{IV} \xrightarrow{-3e} Mn^{VII} \qquad (14)$$

The diagram clearly shows the pε ranges where oxidation and reduction of manganese will occur. It also shows that the poising capacity of the system with respect to pε is maximum

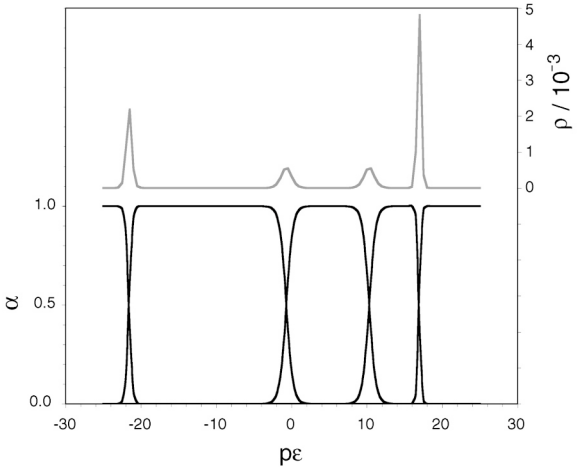

Figure 2. Manganese redox distribution and poising capacity in aqueous solution (Mn_T = 1 mM, pH = 7). The full set of equations used in the calculation is available online.[ω]

when two α functions intersect. The poising capacity of the system is at a relative maximum when the product of oxidant and reductant concentrations is at a maximum. In these respects that system is analogous to weak acid systems.

When performing the calculations for Figure 2, the conditional pε (pε°′) is used to define K, α, and, ρ. The pε°′ accounts for the effect of pH (including acid–base side reactions) and total concentration on the redox potentials for each redox reaction. The full equations used in the calculation are provided online.[W] Notice that the manganese system has 7 electrons transferred, and that two of the steps are multielectron steps. A system with 7 (or fewer) electrons transferred is handled by setting the pε°′ of the 8th dissociation to a large value. In this way the 8th oxidation step never occurs.

Systems with multielectron steps are easily accommodated in the calculations by defining K_j in terms of pε°′ and n, and defining the next $j-1$ dissociation constants as 1.

$$K_j = 10^{n(-\mathrm{p}\varepsilon^{\circ\prime})},\ K_{j+1} = K_{j+2} = \ldots = K_{j+n-1} = 1 \qquad (15)$$

In this case, the value of n is the number of electrons transferred in the single oxidation step (i.e., for $Mn^{IV} \rightarrow Mn^{VII}$, $n = 3$). An example using the manganese system is provided online.[W] The approach defined in eq 15 essentially treats a three-electron transfer as the sum of three single-electron transfers of equivalent free energy change. This approach only yields the correct results, however, when $K << 1$ or pε°′ > 0 for the calculated redox equilibria. As a calculational convenience when working with systems with negative pε°′ values, all pε°′ values are shifted by +30 units; the calculations are then performed and the scale is shifted back for plotting and analysis.

The effect of multiple electron transfers on the α and ρ functions is pronounced. As seen in Figures 2 and 3, the α functions steepen and ρ narrows and increases in height proportional to the square of the number of electrons transferred. The poising capacity also scales linearly with total concentration. The integral of ρ with respect to pε is equal to the number of electrons transferred in the redox reaction (e.g., the area for a two-electron transfer is twice the area for a one-electron transfer.)

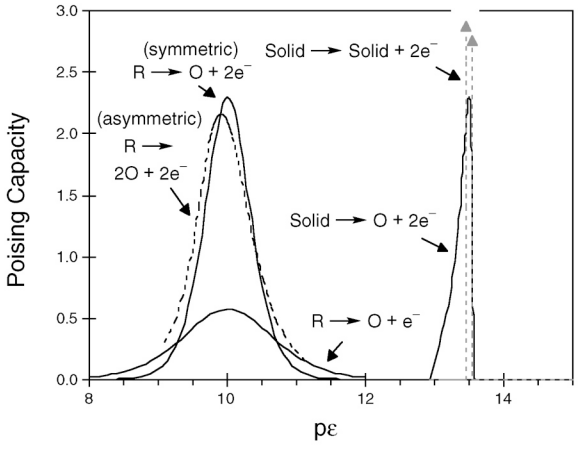

Figure 3. Poising capacity curves for one- and two-electron transfer reactions. The curves on the left are for homogeneous solutions (pε° = 10). The area under the curves reflects the number of electrons transferred (1 or 2). The curves on the right are for solid phases (scaled for plotting, pε° = 13.5). The solid–solid curve is only schematic.

Evaluation of the General Approach

The goal is to describe a general set of equations that can be used easily to describe any redox system as accurately as possible. This then becomes an analysis tool that can be quickly used in classroom lectures or by students to evaluate redox systems. It is informative to look at where the general equations (7–13) work well and where they do not. For redox reactions between symmetrical, homogeneous, solution-phase components the functions for α, η_0, and ρ are in agreement with theory (*6*, *9*). The solutions are exact.

When considering asymmetrical, solution-phase redox reactions such as

$$Cl_2 + 2e^- = 2Cl^- \qquad (16)$$

the equations are not strictly correct, since they do not treat the reaction stoichiometry correctly. The general equations treat chlorine reduction as a simple two-electron reduction. As a result, the functions α, η_0, and ρ are defined on the basis of a mole of Cl atoms rather than a mole of molecules. The pε°′ in this example must also be defined as a function of total Cl_2 atom concentration.[W] The effect of these approximations on ρ is small, as can be seen by comparing the exact solutions for the symmetric and asymmetric ρ curves shown in Figure 3.

The redox speciation of solid phases are also only approximated by the set of general equations. Consider two cases.

Case A:
$$X^{2+} + 2e^- = X(s) \qquad (17)$$

$$\mathrm{p}\varepsilon = \mathrm{p}\varepsilon^\circ + \frac{1}{2}\log\frac{(X^{2+})}{(1)} \qquad (18)$$

Case B:
$$XO_2(s) + 2H^+ + 2e^- = XO(s) + H_2O \qquad (19)$$

$$\mathrm{p}\varepsilon = \mathrm{p}\varepsilon^\circ + \frac{1}{2}\log\frac{(1)(H^+)^2}{(1)(1)} \qquad (20)$$

Case A is a reduction of a solution-phase species to a solid phase. While α, η_0, and ρ functions are clearly defined for this case, the unit activity of the solid phase shifts the functions with respect to pe. The general equations do not predict this shift. Again, the pε°′ in this example is defined as a function of total concentration.[W] Case B is the reduction of a solid phase to form a new solid phase. The activity of $XO_2(s)$ and XO(s) are both unity. The pε is only defined by the pε° and pH. This is a direct consequence of the Gibbs phase rule. For a system described by four components (pH, pε, $Total_X$, (H_2O)) and three phases (solution, $XO_2(s)$, XO(s)), the degrees of freedom are three (pH, $Total_X$, (H_2O)). In other words, the pε is constant when both solids are present in the system. Under these conditions ρ is described by a delta function. The derivative is not defined (it is infinitely large and the peak is infinitely narrow). For case B,

$$\rho = \left|\frac{dC_{ox}}{0}\right| \qquad (21)$$

However, the integral of eq 21 is defined and equals the moles of electrons needed to reduce $XO_2(s)$ to XO(s). The ρ functions for cases A and B are shown in Figure 3. While the general equations do not predict the correct shape of the ρ functions

for solid phases, the center and integral of ρ is correct. For many applications this is more than sufficient.

Redox Titrations

It is interesting to look at the integral of ρ in more detail, since it follows from eqs 12 and 13 that

$$\int_{p\varepsilon_1}^{p\varepsilon_2} \rho_x = \mathrm{TR}\left(\eta_{p\varepsilon_2} - \eta_{p\varepsilon_1}\right) = C_{p\varepsilon_2} - C_{p\varepsilon_1} \qquad (22)$$

where C is the concentration of oxidant or reductant (in electron equivalents) used to "titrate" a given redox system. Equation 22 provides the basis to predict the shape of very complicated titration curves. It is fairly routine to base the solutions for simple redox titrations on segmentation of the titration curve, and explicit expressions for simple redox titrations have been described in this *Journal* by de Levie (*8*). However, it is considerably more difficult to describe the titration curve of a system that undergoes multiple redox transformations. Things get even more complicated when considering a system with multiple redox active species. Such systems include soil or sediment samples that often contain iron, manganese, nitrogen, and sulfur species. Application of eq 22 for predicting titration curves will first be illustrated for the common MnO_4^-–Fe^{2+} system and then for a soil sample.

Consider the titration of MnO_4^- with Fe^{2+}. At a pH below 3 the redox equilibria are

$$Fe^{2+} = Fe^{3+} + e^- \qquad p\varepsilon^{o\prime} = 13 \qquad (23)$$

$$MnO_4^- + 8H^+ + 5e^- = Mn^{2+} + 4H_2O \qquad p\varepsilon^{o\prime} = 20\ (pH \approx 3) \qquad (24)$$

$$MnO_4^- + 8H^+ + 5Fe^{2+} = Mn^{2+} + 4H_2O + 5Fe^{3+}$$

In this example Fe^{2+} is the titrant and MnO_4^- is the analyte. At any point in the titration the total concentration of each species is known and one will be limiting. It is therefore possible to calculate ρ for each species as a function of pε. At any point in the titration, electron balance requires that equivalents of electrons produced by Fe^{2+} oxidation equal the equivalents of electrons consumed by MnO_4^- reduction. In other words, considering eq 22, electron balance requires

$$\int_{p\varepsilon_r}^{p\varepsilon_e} \rho_x = \int_{p\varepsilon_o}^{p\varepsilon_e} \rho_y \qquad (25)$$

where x and y represent the iron and manganese systems, respectively. The solution provides the equilibrium pε ($p\varepsilon_e$) after the addition of titrant and all the limiting reagent has been consumed. The lower boundary condition ($p\varepsilon_r$) is the pε where all iron is in the form of Fe^{2+} (reductant boundary condition), and the upper boundary condition ($p\varepsilon_o$) is a pε where all the manganese is in the form of MnO_4^- (oxidant boundary condition). Figures 4a–4c show the result of this analysis graphically for three different additions of titrant. Figure 5 shows the calculated titration curve. These calculations can be readily performed using a spreadsheet. The calculation involves calculating the poising capacity and integral of poising capacity of the oxidant and the reductant as a function of pε and added titrant. A lookup function is then used to find the pε at the point where the poising capacity integrals are equivalent ($p\varepsilon_e$).

An advantage of the above approach is that the redox titrations of multiple redox reactions can be predicted. An interesting geochemical example is the biologically mediated reaction of organic carbon (reductant) with nitrate, sulfate, Fe^{III} oxide, Mn^{IV} oxide and oxygen (oxidants). The specific redox reactions considered are provided online.[W] Figure 6 shows the electron buffer capacity curves of all species. The concentration of all species was set to 1 mM for intercomparison. Differences in buffer capacity magnitude and position reflect differences in $p\varepsilon^{o\prime}$ and number of electrons

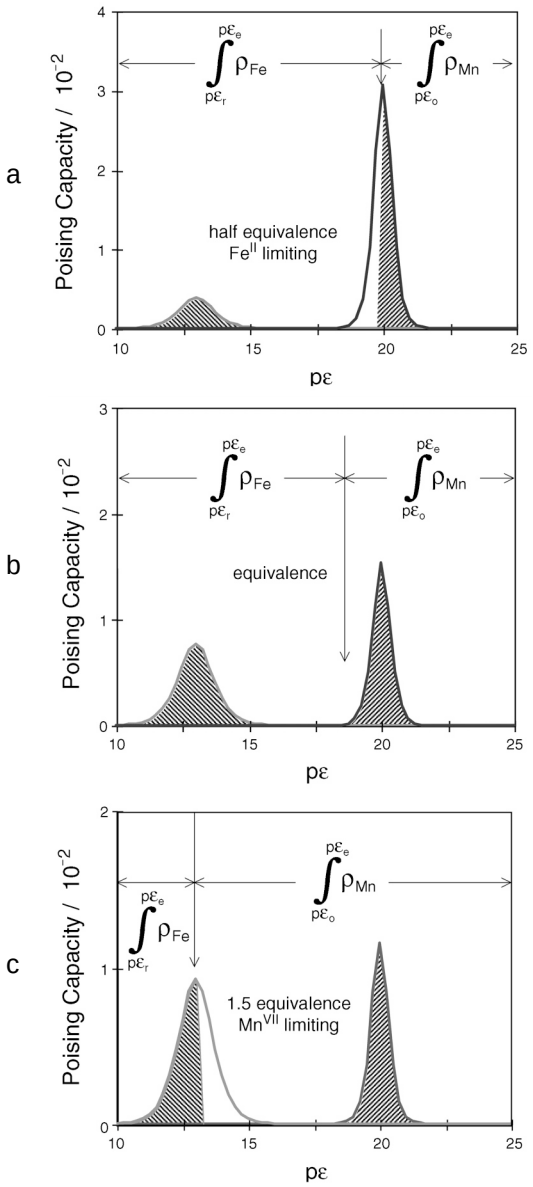

Figure 4. Integrated buffer capacity plots. a: Plot for the Fe^{2+} and MnO_4^- at half way to equivalence (pH ≈ 3). The equilibrium pε is 20. This is the point where the moles of electrons from Fe^{2+} oxidation (area shaded with right diagonal), the limiting reagent, are equal to the moles of electrons consumed by MnO_4^- reduction (area shaded with left diagonal). b: Plot at equivalence. The equilibrium pε is 18.8. c: Plot at 1.5 times equivalence. The equilibrium pε is 13. MnO_4^- is the limiting reagent.

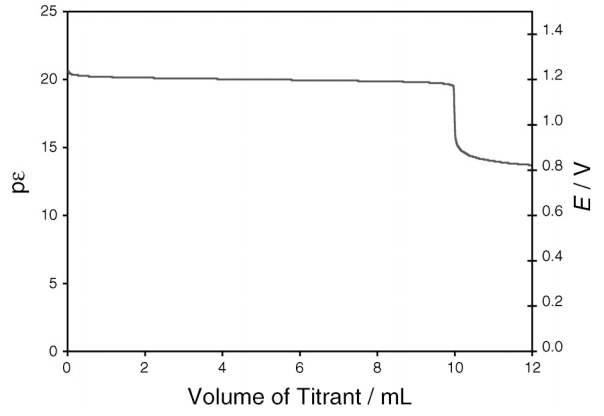

Figure 5. Calculated redox titration of 0.1 L of 1 mM MnO_4^- with 2.5 mM Fe^{2+}.

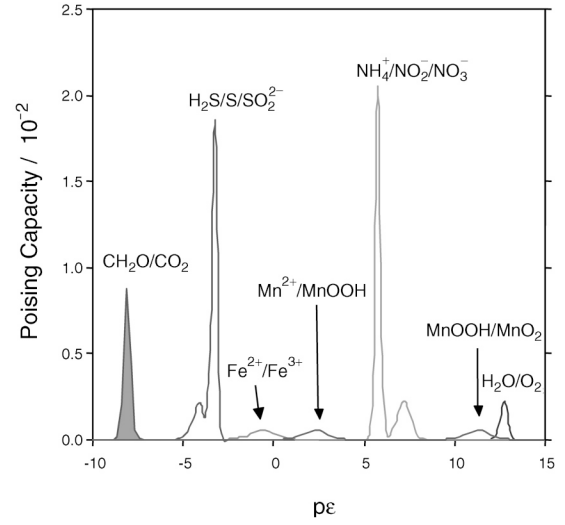

Figure 6. Electron buffer capacity of several geochemically relevant species calculated for pH 7. The concentration of all species is 1 mM except O_2, which is 0.25 mM.

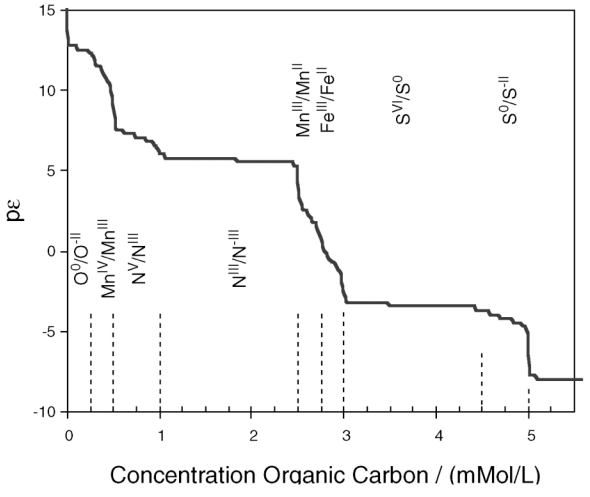

Figure 7. Predicted titration curve for the reduction of oxygen, manganese, nitrogen, iron, and sulfur by organic carbon calculated at pH 7. The concentration of all species is 1 mM except O_2 which is 0.25 mM.

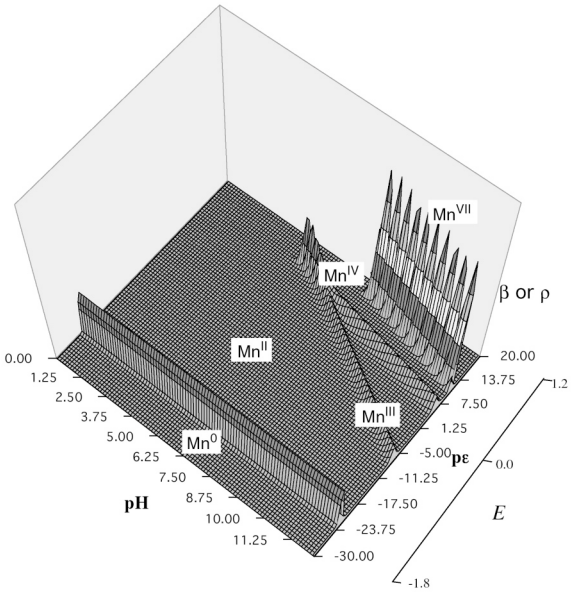

Figure 8. Three-dimensional pε–pH diagram for manganese. Transitions between manganese oxidation states are indicated by peaks in poising capacity. The spikes in the surface are artifacts of the grid spacing. Compare this diagram to Figure 2, which is essentially a slice of the surface at pH 7.

transferred. Considering organic carbon (CH_2O) as the only reductant, the free energy (ΔG) of each redox reaction is proportional to the difference in pε between peaks in buffer capacity. Therefore, over a timescale of days to years (equilibrium control of the system) organic carbon should reduce oxygen first, then manganese(IV), nitrogen(V), iron(III), and sulfur(VI) in that order. In nature, these reactions are biologically mediated. Figure 7 is the predicted titration curve for a soil containing oxygen, manganese, nitrogen, iron, and sulfur "titrated" with organic carbon. A number of investigators have computed similar "titration" curves or reduction capacities for natural systems (*3*, *10*, *11*).

pε–pH Diagrams

A final application of this general model for calculating electron buffer capacity is the generation of pε–pH diagrams. These diagrams are used extensively in geochemistry and environmental chemistry to provide a graphical picture of the redox and pH conditions of a system. They can be calculated automatically by simply plotting electron buffer capacity as a function of pH and pε. Figure 8 is the three-dimensional representation of Figure 2 expanded over a range of pH. The supplemental material contains the equations used the evaluate $p\varepsilon^{o\prime}$ as a function of pH for the manganese system.[W] Notice the similarity to a conventional pε–pH diagram that could be constructed by drawing lines along the maxima in β and ρ.

A practical advantage of these three-dimensional diagrams is that they are easy to create. Using a computer projection system they can be manipulated "live" in front of a class. More importantly, they provide an additional insight into the redox and protonation state of the system by showing a comprehensive picture of the response of the system to additions of oxidant/reductant or acid/base. Combining the

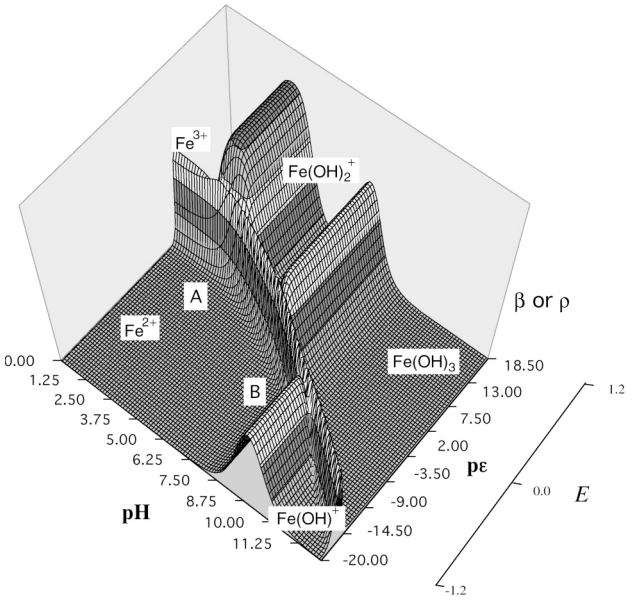

Figure 9. Three-dimensional pε–pH diagram for iron. The transitions between iron oxidation and protonation states are indicated by peaks in buffer capacity. Peaks perpendicular to the pH and pε axis are *only* proton buffer and electron poising capacity, respectively. Peaks along the diagonal represent *both* proton buffer and electron poising capacity. This figure is shown in color on p 1027.

general equations for proton buffer capacity (1–6) with the general equations for poising capacity (10–13), it is straightforward to generate a three-dimensional diagram combining both β and ρ. Figure 9 is a three-dimensional buffer and poising capacity diagram for the Fe^{II}–Fe^{III} system.

As an example of the capabilities of these diagrams, consider starting at point A on Figure 9. This region is poorly buffered with respect to protons or electrons. Adding base to the system will immediately increase the pH to 7.5 (point B), at which point the system becomes buffered. The pε has also decreased. The reason is that the diagram diagonals represent both proton and electron buffer capacities. The addition of base does not add oxidant to the system. Fe^{II} must remain the dominate oxidation state and the pε will drop as the system follows a path to point B.

Implementation

All of the calculations and figures in this paper were calculated using an Excel spreadsheet. These spreadsheets are available online.[W] The advantage of using a general set of equations is that the spreadsheet does not need to be modified for each new redox system. The spreadsheet can be used as a "live" teaching tool in the classroom. As part of the quantitative analysis course at Colby, students develop their own spreadsheet programs to solve solubility, acid–base, and redox problems. Implementation of the expressions described in this work makes for a meaningful integrating exercise for quantitative analysis students.

[W]Supplemental Material

Additional calculations and examples are available in this issue of *JCE Online*.

Literature Cited

1. Pankow, J. F. *Aquatic Chemistry Concepts.*; Lewis: Chelsea, 1991.
2. Morel, F. M. M.; Hering, J. G. *Principles and Application of Aquatic Chemistry*; Wiley: New York, 1993.
3. Stumm, W.; Morgan, J. J. *Aquatic Chemistry: Chemical Equilibria and Rates in Natural Waters*, 3rd ed.; Wiley: New York, 1996.
4. Sillén, L. G. *J. Chem. Educ.* **1952,** *29*, 600.
5. King, D. W.; Kester, D. R. *J. Chem. Educ.* **1990,** *67*, 932–933.
6. de Levie, R. *J. Chem. Educ.* **1999,** *76*, 574–577.
7. Harris, D. C. *Quantitative Chemical Analysis*, 4th ed.; Freeman: New York, 1995.
8. de Levie, R. *J. Chem. Educ.* **1993,** *70*, 209–217.
9. Grundl, T. *Chemosphere* **1994,** *28*, 613–626.
10. *Energetics and Conservative Properties of Redox Systems*; Scott, M.; Morgan, J., Eds.; American Chemical Society: Washington, DC, 1990.
11. Barcelona, M. J.; Holm, T. R. *Envir. Sci. Technol.* **1991,** *25*, 1565–1572.